

A computational model of cation ordering in the magnesioferrite-qandilite ($\text{MgFe}_2\text{O}_4\text{-Mg}_2\text{TiO}_4$) solid solution and its potential application to titanomagnetite ($\text{Fe}_3\text{O}_4\text{-Fe}_2\text{TiO}_4$)

RICHARD J. HARRISON,^{1,*} ERIKA J. PALIN,^{1,†} AND NATASHA PERKS²

¹Department of Earth Sciences, University of Cambridge, Downing Street, Cambridge, CB2 3EQ, U.K.

²Department of Physics, University of Oxford, Parks Road, Oxford, OX1 3PU, U.K.

ABSTRACT

Cation ordering in the magnesioferrite-qandilite ($\text{MgFe}_2\text{O}_4\text{-Mg}_2\text{TiO}_4$) solid solution has been investigated using an interatomic potential model combined with Monte Carlo simulations. The dominant chemical interaction controlling the thermodynamic mixing behavior of the solid solution is a positive nearest-neighbor pairwise interaction between tetrahedrally coordinated Fe^{3+} and octahedrally coordinated Ti^{4+} ($J_{\text{FeTi}}^{\text{TO}}$). The predicted cation distribution evolves gradually from the Néel-Chevalier model to the Akimoto model as a function of increasing $J_{\text{FeTi}}^{\text{TO}}$, with $J_{\text{FeTi}}^{\text{TO}} = 1000 \pm 100$ K providing an adequate description of both the temperature and composition dependence of the cation distribution and the presence of a miscibility gap. Although Mg is a good analog of Fe^{2+} in end-member spinels, a comparison of model predictions for $\text{MgFe}_2\text{O}_4\text{-Mg}_2\text{TiO}_4$ with observed cation ordering behavior in titanomagnetite ($\text{Fe}_3\text{O}_4\text{-Fe}_2\text{TiO}_4$) demonstrates that the analog breaks down for Fe_3O_4 -rich compositions, where a value of $J_{\text{FeTi}}^{\text{TO}}$ closer to zero is needed to explain the observed cation distribution. It is proposed that screening of Ti^{4+} by mobile charge carriers on the octahedral sublattice is responsible for the dramatic reduction in $J_{\text{FeTi}}^{\text{TO}}$. If confirmed, this conclusion will have significant implications for attempts to create a realistic thermodynamic model of titanomagnetite.

Keywords: Magnesioferrite, qandilite, titanomagnetite, cation distribution, computer simulations

INTRODUCTION

The titanomagnetite solid solution between magnetite (Fe_3O_4) and ulvöspinel (Fe_2TiO_4) is the dominant carrier of magnetic remanence in nature and is of central importance to paleomagnetic, rock magnetic, and mineral magnetic studies. Both end-members adopt the cubic inverse spinel structure at room temperature, with cations occupying two distinct types of crystallographic site (tetrahedral and octahedral). The distribution of Fe^{3+} , Fe^{2+} , and Ti^{4+} cations between tetrahedral and octahedral sites has a profound impact on the intrinsic magnetic properties of titanomagnetite. The presence of tetrahedral Fe^{2+} is of particular importance, as this has been linked to large increases in both magnetocrystalline anisotropy and magnetostriction due to a dynamic Jahn-Teller distortion (Kakol et al. 1991a, 1991b; Church et al. 2011). However, despite numerous studies performed over many years with a range of increasingly sophisticated analysis techniques (see Pearce et al. 2010 for a review), there is still no consensus regarding the temperature and composition dependence of the cation distribution in titanomagnetite. For example, two of the most recent and detailed studies [Bosi et al. (2009) using X-ray single-crystal diffraction and Pearce et al. 2010 using X-ray magnetic circular dichroism] present results that are at opposite extremes of the range of previously reported cation distributions and that disagree dramatically in their assessment of when Fe^{2+} first enters the tetrahedral site.

A complicating factor in titanomagnetite is that Fe^{2+} and Fe^{3+} differ only by a single, highly mobile 3d electron, which not only makes distinguishing the two cations an experimental challenge but also makes computational studies more difficult due to the problem of deciding how the excess electron density associated with Fe^{2+} should be distributed across the available Fe sites. Given these complexities, it becomes a worthwhile exercise to consider the magnesioferrite-qandilite ($\text{MgFe}_2\text{O}_4\text{-Mg}_2\text{TiO}_4$) solid solution—a potential analog of titanomagnetite in which the Fe^{2+} cation is entirely replaced by Mg^{2+} . It has long been established that Mg^{2+} is a good analog for Fe^{2+} in end-member spinels, with the substitution of Mg^{2+} for Fe^{2+} having little effect on temperature-dependent cation distributions (Harrison and Putnis 1999a) and spinel solid solutions involving exchange of Mg^{2+} and Fe^{2+} behaving in a manner that is close to ideal (Trestman-Matts et al. 1984; Nell et al. 1989; Andreozzi and Lucchesi 2002; Palin and Harrison 2007a). The $\text{MgFe}_2\text{O}_4\text{-Mg}_2\text{TiO}_4$ solid solution offers, therefore, the possibility to study cation ordering in a system that is closely analogous to titanomagnetite, yet: (1) allows the distribution of Mg^{2+} and Fe^{3+} cations to be determined reliably using X-ray powder diffraction; (2) permits the high-temperature distribution to be quenched without significant cation redistribution; (3) enables sample synthesis and analysis to be performed in air at high temperatures without fear of oxidation; and (4) lacks the computational complexities associated with mobile electronic charge.

The main focus of this paper is the development of an atomistic model of cation ordering in $\text{MgFe}_2\text{O}_4\text{-Mg}_2\text{TiO}_4$. The computational approach, outlined in the next section, builds on

* E-mail: rjh40@esc.cam.ac.uk

† Present address: Meteorological Office Hadley Centre, FitzRoy Road, Exeter, EX1 3PB, U.K.

that developed by Palin and Harrison (2007b) and Palin et al. (2008) for the end-members MgFe₂O₄ and Mg₂TiO₄, combined with the extension of the method to binary spinel solid solutions by Palin and Harrison (2007a). Application of the method to MgFe₂O₄-Mg₂TiO₄ is described and comparisons are made between MgFe₂O₄-Mg₂TiO₄ and Fe₃O₄-Fe₂TiO₄. Possible reasons for the observed differences between the two systems are explored. Our conclusions provide new insight into the nature of cation ordering in titanomagnetite, and point the way forward for future computational studies of this important magnetic mineral.

DEVELOPMENT OF THE ATOMISTIC MODEL

Theory

The atomistic model used here is based on the J formalism described by Bosenick et al. (2001) and Palin and Harrison (2007b). The total energy, E , of a network of interacting cations can be expressed as a sum of pairwise cation-cation interaction energies. For two species A and B mixing on a network of identical sites, $E = N_{AA}E_{AA} + N_{BB}E_{BB} + N_{AB}E_{AB}$, where E_{AA} , E_{BB} , and E_{AB} are the energies associated with A-A, B-B, and A-B nearest neighbor pairs, and N_{AA} , N_{BB} , and N_{AB} are the number of A-A, B-B, and A-B pairs in the network. The interdependence of N_{AA} , N_{BB} , and N_{AB} allows this expression to be rewritten solely in terms of the number of unlike cation pairs in the network, $E = E_0 + N_{AB}J$, where E_0 is a constant and $J = E_{AB} - 1/2(E_{AA} + E_{BB})$. The sign of J determines the ordering behavior of the A and B cations: positive values favor A-A and B-B neighbors, leading to chemical clustering; negative values favor A-B neighbors, leading to cation ordering. Interaction parameters describing the energy of more distant neighbor pairs can be defined in the same way and summed to give the total energy of the system. In the case of spinel, where cations are distributed across two networks of symmetrically distinct sites (i.e., the tetrahedral [T] and octahedral [O] sublattices), an additional site preference energy (a.k.a. chemical potential, μ) is required to complete the total energy. Chemical potential terms can be written $E = \mu N_A^T$, where N_A^T is the number of A atoms sitting on the T sublattice. The sign of μ dictates the site preference of A: a positive value indicates an O site preference, a negative value a T site preference. Using static lattice empirical potential calculations, Palin and Harrison (2007b) determined μ and J for T-T, O-O, and T-O interactions out to fourth nearest neighbors in a range of 2-3 end-member spinels, including MgFe₂O₄. Using a combination of static lattice empirical potential and ab initio calculations, Palin et al. (2008) performed a similar exercise for the 2-4 spinel Mg₂TiO₄. The extension of the J formalism to the binary spinel solid solution MgAl₂O₄-FeAl₂O₄ is described by Palin and Harrison (2007a). Adaptation of this method to MgFe₂O₄-Mg₂TiO₄ is described below.

Magnesioferrite-qandilite (MgFe₂O₄)_{1-M}(Mg₂TiO₄)_M is a binary system consisting of two inverse spinels. The cation distribution between T and O sites can be written as

	T	O	Sum
Mg ²⁺	1 - x - y	M + x + y	1 + M
Fe ³⁺	x	2 - 2M - x	2 - 2M
Ti ⁴⁺	y	M - y	M
Sum	1	2	3

where x and y are cation distribution parameters and M is the mole fraction of Mg₂TiO₄. As shown by Palin and Harrison (2007a), the total energy of such a system can formally be expressed as a sum of pairwise cation-cation interaction parameters and chemical potentials

$$\begin{aligned}
 E = & N_{\text{MgFe}}^{\text{TT}} J_{\text{MgFe}}^{\text{TT}} + N_{\text{MgTi}}^{\text{TT}} J_{\text{MgTi}}^{\text{TT}} + N_{\text{FeTi}}^{\text{TT}} J_{\text{FeTi}}^{\text{TT}} \\
 & + N_{\text{MgFe}}^{\text{OO}} J_{\text{MgFe}}^{\text{OO}} + N_{\text{MgTi}}^{\text{OO}} J_{\text{MgTi}}^{\text{OO}} + N_{\text{FeTi}}^{\text{OO}} J_{\text{FeTi}}^{\text{OO}} \\
 & + N_{\text{MgFe}}^{\text{TO}} J_{\text{MgFe}}^{\text{TO}} + N_{\text{MgTi}}^{\text{TO}} J_{\text{MgTi}}^{\text{TO}} + N_{\text{FeTi}}^{\text{TO}} J_{\text{FeTi}}^{\text{TO}} \\
 & + \mu_x x + \mu_y y + \mu_M M \\
 & + E_0
 \end{aligned} \tag{1}$$

where $N_{\text{MgFe}}^{\text{TT}}$, etc., is the number of Mg²⁺-Fe³⁺ cation pairs of a given type and $J_{\text{MgFe}}^{\text{TT}}$, etc., is the corresponding interaction parameter. E_0 is a constant that plays no role in determining the cation distribution. There is a chemical potential term corresponding to each of the independent variables defining the cation distribution (x , y , and M). The μ_M chemical potential produces a linear variation of total energy with bulk composition of the system, and plays no role in determining either the cation distribution or the excess thermodynamic mixing properties of the solid solution. The choice of variables x and y to describe the cation distribution is somewhat arbitrary. However, since Fe³⁺ and Ti⁴⁺ are absent from the Mg₂TiO₄ and MgFe₂O₄ end-members, respectively, this choice allows μ_x and μ_y to be equated with the chemical potentials already determined for each end-member. Implicit in Equation 1 is that interactions are summed over first, second, third, and fourth nearest neighbor interactions, as described by Palin and Harrison (2007b).

Determination of the solid-solution J parameters

The only energy terms in Equation 1 that are not already known from studies of the end-members are the Fe³⁺-Ti⁴⁺ cation-cation interaction parameters $J_{\text{FeTi}}^{\text{TT}}$, $J_{\text{FeTi}}^{\text{OO}}$, and $J_{\text{FeTi}}^{\text{TO}}$. As with our previous work, static lattice energy calculations using empirical interatomic potentials are used to estimate values for the unknown J s. The interatomic potentials have the Buckingham form

$$E = A \exp(-r/\rho) - \frac{C}{r^6} \tag{2}$$

where A , ρ , and C are constants, and the value of A depends on the coordination of the atom. Formal charges were used for all species, and the potential parameters used were obtained from previous work on the end-members MgFe₂O₄ and Mg₂TiO₄ (Palin and Harrison 2007b; Palin et al. 2008). We examined 16 different compositions across the join, i.e., $M = 0, 1/16, \dots, 1$. A $2 \times 2 \times 2$ supercell of the spinel structure was created and the cations were placed randomly on the available T and O sites in proportions appropriate to the chosen values of x , y , and M . Given that the amount of Ti⁴⁺ on tetrahedral sites is observed by experiment to be negligible at all compositions and temperatures (de Grave et al. 1975), we chose to place Ti⁴⁺ cations exclusively on the octahedral sublattice (i.e., $y = 0$). This decision was taken to minimize undue bias in the derived interaction parameters by ensuring that all of the generated configurations were physically

achievable by the real system. A total of 217 configurations were created. Each configuration was relaxed with respect to both lattice parameters and atomic positions at constant pressure using the program GULP (Gale 1997; Gale and Rohl 2003). The set of 217 optimized lattice energies were then used to calculate values for all J 's and μ 's using the least-squares optimization method of Bosenick et al. (2001). Given the lack of tetrahedral Ti^{4+} , $J_{\text{MgTi}}^{\text{TT}}$, and $J_{\text{FeTi}}^{\text{TT}}$ were not included in the optimization procedure. All other parameters were allowed to vary.

Results of the J optimization procedure are displayed in Figure 1. The J_{MgTi} and J_{MgFe} parameters obtained here display the same systematics observed in the end-member studies (Palin and Harrison 2007b; Palin et al. 2008). The first nearest neighbor interactions are dominant, and all statistically significant interaction parameters are negative, indicating that Mg^{2+} - Ti^{4+} and Mg^{2+} - Fe^{3+} cation pairs are energetically favorable. J_{MgTi} parameters are typically larger than the corresponding J_{MgFe} parameters. This is due to the larger contrast in cation charge for Mg^{2+} - Ti^{4+} pairs compared to Mg^{2+} - Fe^{3+} pairs, which leads to a larger electrostatic contribution to the interaction energy. The values of J_{MgTi} are similar to those obtained by Palin et al. (2008) for end-member Mg_2TiO_4 . Value of J_{MgFe} , however, are significantly larger than those reported by Palin and Harrison (2007b) for end-member MgFe_2O_4 . This is due to the use of a formal charge of -2 for O atoms in this study, rather than the value of -1.65 used by Palin and Harrison (2007b). In the following, we adopt the simplest assumption that J_{MgTi} and J_{MgFe} are independent of bulk composition and equal to those derived for the end-members. This ensures, at least, that the model reproduces the observed end-member behavior.

The optimized results for J_{FeTi} interactions indicate that the dominant interaction in the solid solution is the first nearest neighbor interaction between Fe^{3+} cations on tetrahedral sites and Ti^{4+} cations on octahedral sites (referred to from now on as $J_{\text{FeTi}}^{\text{TO}}$).

All other J_{FeTi} interactions are within two standard deviations of zero. The fitted value of $J_{\text{FeTi}}^{\text{TO}}$ (1828 ± 286 K) is large and positive, indicating that Fe^{3+} - Ti^{4+} TO pairs are energetically unfavourable and that the system will attempt to minimize the number of such pairs in the solid solution. This result compares favorably with the hematite-ilmenite (Fe_2O_3 - FeTiO_3) system, where first nearest neighbor interactions between Fe^{3+} and Ti^{4+} were also found to be positive (Harrison et al. 2000; Harrison 2006).

J values extracted using static lattice empirical potential calculations provide valuable insight into the sign and relative importance of different cation-cation interactions, but often produce only approximate agreement with experimental observations. The prediction that there is only one dominant interaction in the solid solution greatly simplifies attempts to obtain a physically realistic model that reproduces the experimental data. In "Application to MgFe_2O_4 - Mg_2TiO_4 ," we explore the thermodynamic behavior of the system as a function of increasing $J_{\text{FeTi}}^{\text{TO}}$ and compare the predicted results with experimental observations to obtain an estimate of the most likely value of this parameter in the real system.

Monte Carlo simulations

Monte Carlo (MC) simulations were used to determine the equilibrium cation distribution as a function of temperature and composition, according to the methods outlined by Harrison (2006). A $4 \times 4 \times 4$ supercell of the spinel structure was created, containing a total of 1536 cation sites (512 tetrahedral and 1024 octahedral) with periodic boundary conditions. Individual simulations were performed with a fixed bulk composition varying between $0 \leq M \leq 1$ in steps of either 0.1 or 0.2. Starting configurations were created by distributing Ti^{4+} randomly over the octahedral sublattice and then distributing Mg^{2+} and Fe^{3+} randomly over the remaining T and O sites. Note that Ti^{4+} was not constrained to sit exclusively on O sites during the subse-

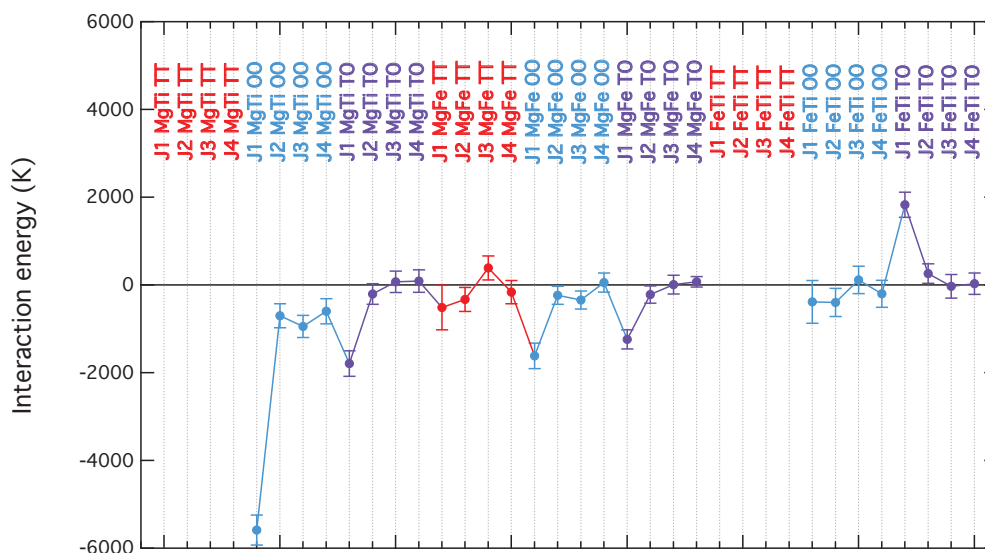


FIGURE 1. Cation-cation interaction energies extracted from static lattice energy calculations using the optimization procedure of Bosenick et al. (2001). J_1 , J_2 , J_3 , and J_4 refer to first, second, third, and fourth nearest neighbor interactions. TT, OO, and TO refer to tetrahedral-tetrahedral, octahedral-octahedral, and tetrahedral-octahedral interactions, respectively. TT interactions involving Ti^{4+} are absent, since Ti^{4+} was placed on octahedral sites only. (Color online.)

quent simulations. Simulations were performed on cooling from 1750 to 250 K in steps of 250 K. Each simulation ran for a total of 2×10^7 cation swaps (that is, 10^7 equilibration steps and 10^7 production steps).

The J and μ parameters used in the simulations are listed in Table 1. J_{MgTi} , J_{MgFe} , μ_x , and μ_y were taken directly from the end-member studies of Palin and Harrison (2007b) and Palin et al. (2008) (note, however, the change in sign of μ_x , since we chose here to define the chemical potential energy using the number of Ti^{4+} cations on T rather than O sites). In both end-member studies, the parameters were optimized to give a good description of the observed ordering behavior. The only additional parameter used in this study is the first nearest-neighbor $J_{\text{FeTi}}^{\text{TO}}$ interaction. Parameters E_0 and μ_{M} in Equation 1 have no effect on the cation distribution or excess thermodynamic properties and were not used in the MC simulations.

APPLICATION TO $\text{MgFe}_2\text{O}_4\text{-Mg}_2\text{TiO}_4$

Cation ordering as a function of temperature, M and $J_{\text{FeTi}}^{\text{TO}}$

Simulations were performed for $J_{\text{FeTi}}^{\text{TO}}$ values ranging from 0 to 1500 K. In all cases, Ti^{4+} was found almost exclusively on octahedral sites. The maximum amount of Ti^{4+} on tetrahedral sites was $y = 0.026$ (for $T = 1750$ K, $M = 0.8$, and $J_{\text{FeTi}}^{\text{TO}} = 0$). This amount of tetrahedral Ti^{4+} is consistent with experimental observations of Mg_2TiO_4 at high temperatures (O'Neill et al. 2003). Given that $y \sim 0$, the distribution of all other cations can be defined by a single order parameter, x . We have chosen to summarize the MC results in Figure 2 by plotting the number of tetrahedral Mg^{2+} cations per formula unit ($\text{Mg}^{\text{T}} \sim 1 - x$) as a function of M . Simulated results are shown as black solid lines. The uppermost curve in each figure shows the highest temperature simulation (1750 K), the lowermost curve shows the lowest temperature simulation (250 K).

To aid the discussion, dashed lines in Figure 2 show four

TABLE 1. Cation-cation interaction parameters and chemical potentials of the atomistic model

	Energy (K)	Reference
J1 MgTi TT	728	Palin et al. (2008)
J2 MgTi TT	0	Palin et al. (2008)
J3 MgTi TT	0	Palin et al. (2008)
J4 MgTi TT	0	Palin et al. (2008)
J1 MgTi OO	-3102	Palin et al. (2008)
J2 MgTi OO	0	Palin et al. (2008)
J3 MgTi OO	-272	Palin et al. (2008)
J4 MgTi OO	-116	Palin et al. (2008)
J1 MgTi TO	-1706	Palin et al. (2008)
J2 MgTi TO	0	Palin et al. (2008)
J3 MgTi TO	0	Palin et al. (2008)
J4 MgTi TO	0	Palin et al. (2008)
J1 MgFe TT	-164	Palin and Harrison (2007a)
J2 MgFe TT	-68	Palin and Harrison (2007a)
J3 MgFe TT	-45	Palin and Harrison (2007a)
J4 MgFe TT	-5	Palin and Harrison (2007a)
J1 MgFe OO	-340	Palin and Harrison (2007a)
J2 MgFe OO	-51	Palin and Harrison (2007a)
J3 MgFe OO	-62	Palin and Harrison (2007a)
J4 MgFe OO	-28	Palin and Harrison (2007a)
J1 MgFe TO	-313	Palin and Harrison (2007a)
J2 MgFe TO	-144	Palin and Harrison (2007a)
J3 MgFe TO	-53	Palin and Harrison (2007a)
J4 MgFe TO	-19	Palin and Harrison (2007a)
J1 FeTi TO	0-1500	This study
μ_x	-950	Palin and Harrison (2007a)
μ_y	-1114	Palin et al. (2008)

reference cation distribution models. Each of the four models assumes that Ti^{4+} occurs exclusively on octahedral sites. The ‘‘Random’’ model corresponds to a random distribution of Mg^{2+} and Fe^{3+} across T and O sites. The ‘‘Akimoto’’ model is analogous to that proposed by Akimoto (1954) for titanomagnetite, and corresponds to a linear variation in tetrahedral Mg^{2+} as a function of M . The ‘‘Kakol’’ model is analogous to that proposed by Kakol et al. (1991b) for titanomagnetite, whereby no tetrahedral Mg^{2+} appears until $M > 0.2$. The ‘‘Néel-Chevalier’’ model is analogous to that proposed by Néel (1955) and Chevalier et al. (1955) for titanomagnetite, whereby no tetrahedral Mg^{2+} appears until $M > 0.5$.

For $0 \leq J_{\text{FeTi}}^{\text{TO}} \leq 250$ K, the low-temperature state of the system corresponds to the Néel-Chevalier model (Figs. 2a and 2b). No Mg^{2+} enters the tetrahedral sites until $M > 0.5$, at which point all octahedral Fe^{3+} is used up and there is no choice but to place additional Mg^{2+} on tetrahedral sites. The tetrahedral preference of Fe^{3+} over Mg^{2+} is a consequence of the negative value of μ_x (Table 1), which dictates that total energy is lowered by increasing tetrahedral Fe^{3+} at the expense of tetrahedral Mg^{2+} (given that Ti^{4+} strongly favors octahedral sites). Increasing temperature leads to increasing Mg^{T} . For $0 < M \leq 0.5$, the temperature dependence of Mg^{T} tracks that observed in end-member MgFe_2O_4 (O'Neill et al. 1992; Antao et al. 2005). The temperature dependence of Mg^{T} diminishes for $M > 0.5$ and disappears entirely for $M > 0.8$.

For $J_{\text{FeTi}}^{\text{TO}} = 500$ K, there is a marked change in the low-temperature state of the system, with Mg^{2+} entering tetrahedral sites for all $M > 0$ (Fig. 2c). The system adopts a mixed cation distribution that is close to the Néel-Chevalier model for $M > 0.8$ but is closer to the Akimoto model for $M < 0.2$. For $750 \leq J_{\text{FeTi}}^{\text{TO}} \leq 1000$ K, the low-temperature state moves closer to the Akimoto model, with an approximately linear variation of Mg^{T} with M (Figs. 2d–2f). For $0 < M < 0.5$ the temperature-dependence of Mg^{T} is bounded by the Random model at high T and the Akimoto model at low T . For $M > 0.5$, Mg^{T} remains close to the Akimoto/Random models and there is little temperature dependence (these two models become virtually indistinguishable as M tends to 1). For $J_{\text{FeTi}}^{\text{TO}} = 1100$ K, the cation distribution follows the Random model for $0.4 \leq M \leq 1$ (Fig. 2g). For $J_{\text{FeTi}}^{\text{TO}} > 1100$ K we begin to see Mg^{T} values that exceed the Random model, implying that Mg^{2+} now has a tetrahedral preference relative to Fe^{3+} .

Comparison with experimental observations

Experimental measurements of the cation distribution in $\text{MgFe}_2\text{O}_4\text{-Mg}_2\text{TiO}_4$ have been reported by Tellier (1967) and de Grave et al. (1975). The results of de Grave et al. (1975) are shown in Figure 3a for two suites of samples: the first was quenched from 1373 K in water (upward triangles) and the second was cooled slowly from 1373 K at a rate of 1 K per min (downward triangles). Also shown in Figure 3a are new results from our own experimental work on this system (circles). Details of the experimental work will be presented in detail elsewhere. Samples were synthesized in air at 1400 °C from mixtures of Fe_2O_3 and TiO_2 and then furnace cooled. Cation distributions were obtained by Rietveld refinement of X-ray powder diffraction patterns, and are in excellent agreement with those of de Grave et al. (1975). For $0 \leq M \leq 0.5$, the observed cation distributions fall in between the Random and Akimoto models, with

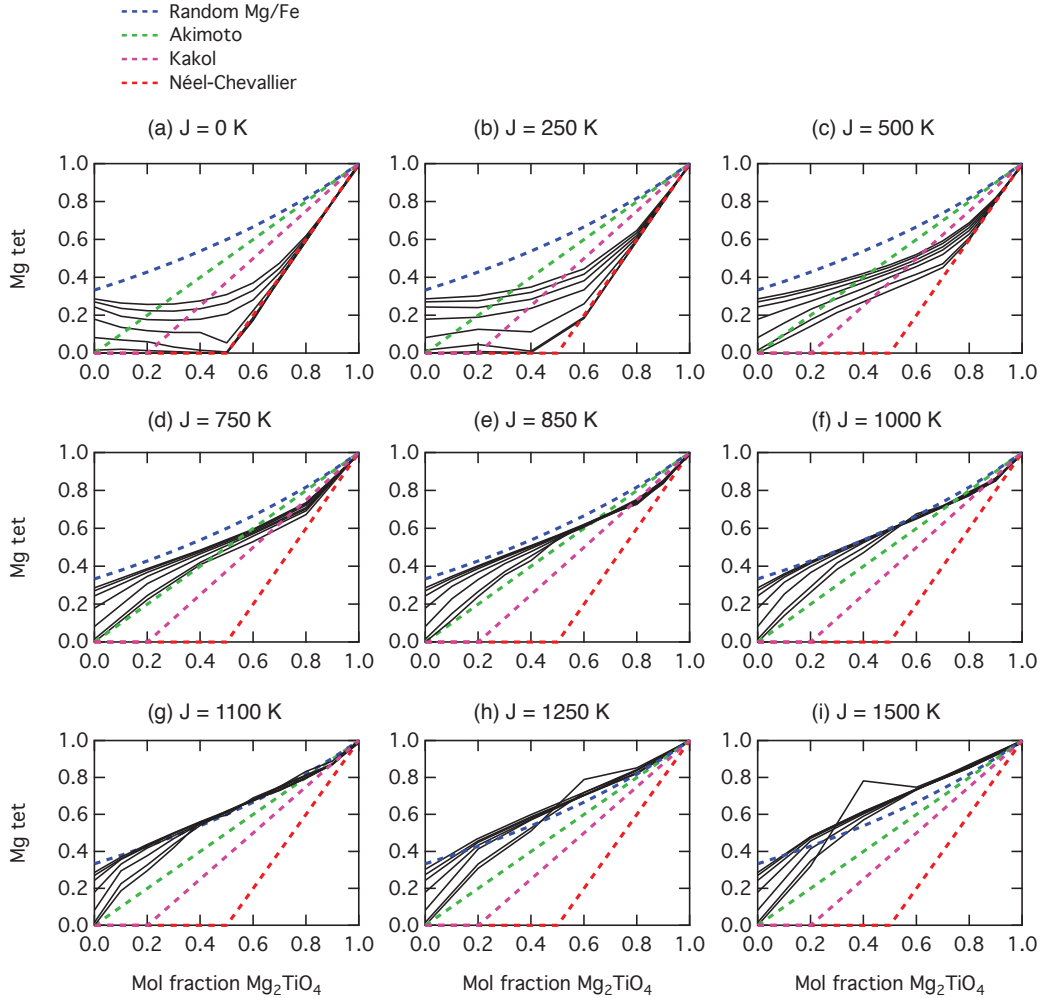


FIGURE 2. Summary of MC results obtained for MgFe_2O_4 - Mg_2TiO_4 with $J_{\text{FeTi}}^{\text{TO}}$ equal to (a) 0 K, (b) 250 K, (c) 500 K, (d) 750 K, (e) 850 K, (f) 1000 K, (g) 1100 K, (h) 1250 K, and (i) 1500 K. Solid curves show the results of MC simulations performed at temperatures of (from upper to lower curves) 1750, 1500, 1250, 1000, 750, 500, and 250 K. Dashed lines show reference cation distribution models (from upper to lower dashed curves): Random, Akimoto, Kakol, and Néel-Chevallier. (Color online.)

the quenched samples falling closer to the Random model and slowly cooled samples falling closer to the Akimoto model. For $M > 0.5$ the observed cation distribution follows the Random model. Comparing Figure 3a with the results of MC simulations (Fig. 2), it appears that the atomistic model with $J_{\text{FeTi}}^{\text{TO}} = 1000 \pm 100$ K provides an adequate description of both the temperature and composition dependence of cation ordering in this system (Fig. 2f). This value of $J_{\text{FeTi}}^{\text{TO}}$ is of the same order of magnitude as that predicted by the interatomic potential calculations presented earlier ($J_{\text{FeTi}}^{\text{TO}} = 1828 \pm 286$ K).

Perhaps a more rigorous method of presenting the experimental data follows from the thermodynamic model of binary spinel solid solutions described by O'Neill and Navrotsky (1984). Assuming that Ti^{4+} sits on O sites exclusively ($\gamma = 0$), thermodynamic equilibrium with respect to the amount of Fe^{3+} on T sites (x) can be expressed in the for

$$-RT \ln(K) = \alpha + 2\beta x \quad (3)$$

$$\ln(K) = \ln \left(\frac{x(M+x)}{(1-x)(2-2M-x)} \right)$$

where α and β are coefficients describing the enthalpy variation as a function of x ($H = \alpha x + \beta x^2$). According to Equation 3, a plot of $-RT \ln(K)$ vs. x should yield a straight line with intercept α and slope 2β . To plot the data in this form, we require an estimate for the temperature at which the cation distribution has been equilibrated. For the quenched samples of de Grave et al. (1975) and Tellier (1967) we have assumed that the equilibration temperature is equal to the quench temperature (1373 K). For our own samples and the slowly cooled samples of de Grave et

al. (1975) we use an estimated equilibration temperature of 667 K, which corresponds to the temperature at which the observed cation distribution in end-member MgFe_2O_4 is equal to the predicted cation distribution according to the thermodynamic model of O'Neill et al. (1992). The resulting plot is shown in Figure 4a. The dashed line shows the predicted behavior according to the O'Neill and Navrotsky (1984) model, with the values of $\alpha = 26.6$ kJ/mol and $\beta = -21.7$ kJ/mol obtained by fitting cation distribution data for end-member MgFe_2O_4 (O'Neill et al. 1992).

Although there is good agreement with the O'Neill-Navrotsky model for $0.7 < x < 1$ (which corresponds mainly to the range of x values in end-member MgFe_2O_4), there is dramatic deviation from linear behavior for $x < 0.7$ (which corresponds mainly to the range of x values in the solid solution). Solid curves in Figure 4a show the calculated behavior using the atomistic model with $J_{\text{FeTi}}^{\text{TO}} = 1000$ K. The lowermost curve corresponds to highest temperature (1750 K) and the uppermost curve to the lowest temperature (250 K). Agreement between observed

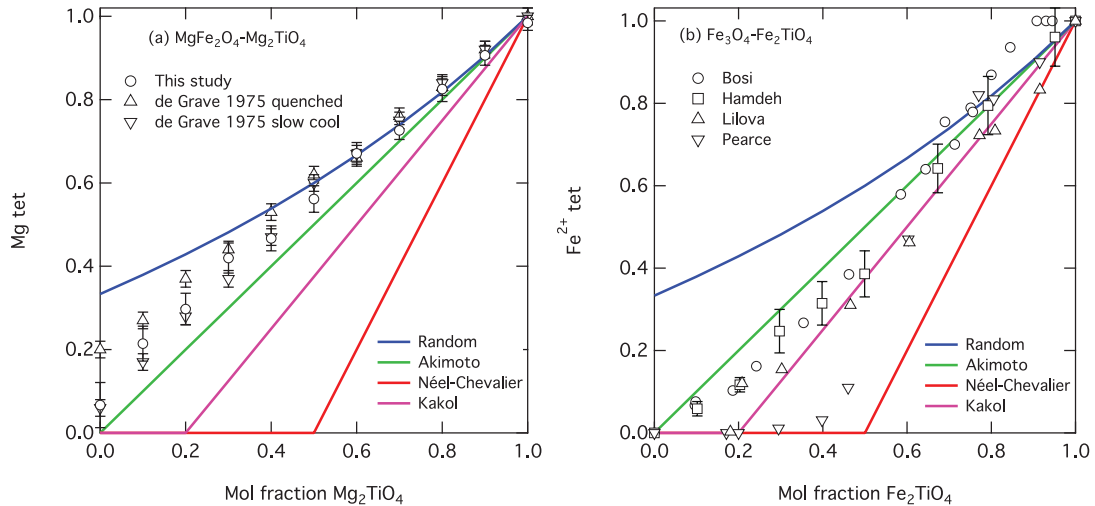


FIGURE 3. (a) Experimentally determined cation distributions in MgFe_2O_4 - Mg_2TiO_4 . Open circles are data from this study. Triangles are quenched and slowly cooled samples from de Grave et al. (1975). (b) Experimentally determined cation distributions in Fe_3O_4 - Fe_2TiO_4 . Data are from Bosi et al. (2009) (circles), Hamdeh et al. (1999) (squares), Lilova et al. (2012) (upward triangles), and Pearce et al. (2010) (downward triangles). Solid lines in a and b show reference cation distribution models (from upper to lower): Random, Akimoto, Néel-Chevalier, and Kakol. (Color online.)

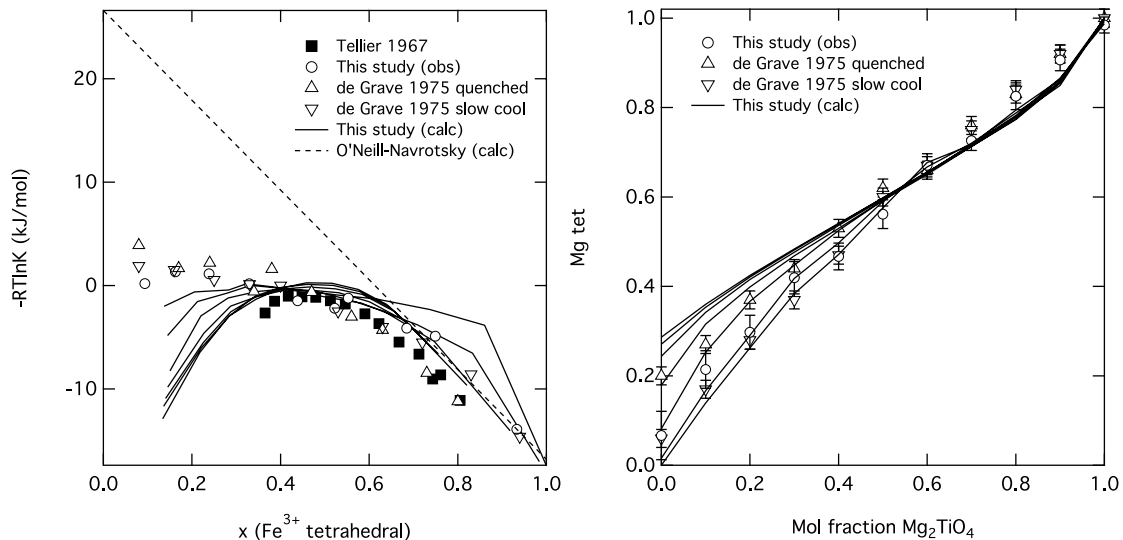


FIGURE 4. (a) Cation distributions in MgFe_2O_4 - Mg_2TiO_4 plotted in the form of Equation 3 (O'Neill and Navrotsky 1984). Data shown from this study (open circles), Tellier (1967) (closed squares), and de Grave et al. (1975) (open triangles). Solid curves show the results of MC simulations with $J_{\text{FeTi}}^{\text{TO}} = 1000$ K at temperatures of (from lower to upper curves) 1750, 1500, 1250, 1000, 750, 500, and 250 K. Dashed line shows the prediction of the O'Neill and Navrotsky (1984) model using Equation 3 with values of $\alpha = 26.6$ kJ/mol and $\beta = -21.7$ kJ/mol (O'Neill et al. 1992). (b) Direct comparison of observed cation distributions in MgFe_2O_4 - Mg_2TiO_4 with results of MC simulations with $J_{\text{FeTi}}^{\text{TO}} = 1000$ K at temperatures of (from upper to lower curves) 1750, 1500, 1250, 1000, 750, 500, and 250 K.

and calculated behavior is much improved with respect to the O'Neill-Navrotsky model. In particular, the predicted curvature of the $-RT\ln(K)$ vs. x plot agrees very well with the data of Tellier (1967) (solid squares). Agreement appears to be poorest for small values of x , corresponding to compositions close to Mg_2TiO_4 . However, comparing the observed and calculated distributions directly (Fig. 4b), we see that this disagreement is perhaps over emphasized by Equation 3.

Enthalpies of mixing and immiscibility in the solid solution

An independent check of the calibration of the atomistic model can be performed by comparing the calculated and observed enthalpies of mixing (ΔH_{mix}). ΔH_{mix} was calculated by subtracting the MC energy of a mechanical mixture of the end-members from the MC energy of the solid solution (Fig. 5). At 1750 K (uppermost curve) there is a positive symmetrical enthalpy of mixing that can be described by a regular solution model $\Delta H_{\text{mix}} = WM(1 - M)$ with $W = 24$ kJ/mol. As far as we are aware, there are no published reports of ΔH_{mix} data for MgFe_2O_4 - Mg_2TiO_4 . However, in the context of this comparative study, it is useful to compare our predicted curves with recent calorimetric measurements of the titanomagnetite solid solution (Lilova et al. 2012). Drop solution calorimetry data for a suite of titanomagnetites synthesized at 1173 K are plotted as closed circles in Figure 5. Their data correspond to a regular solution model with $W = 22.60 \pm 8.46$ kJ/mol, which is well within the range of predicted values for the Mg analog system.

Significant changes in the magnitude, symmetry, and curvature of ΔH_{mix} occur at lower simulation temperatures. At 1250 K there is a flattening of the ΔH_{mix} curve, and below 1000 K the ΔH_{mix} curves become linear in the central region. This type of

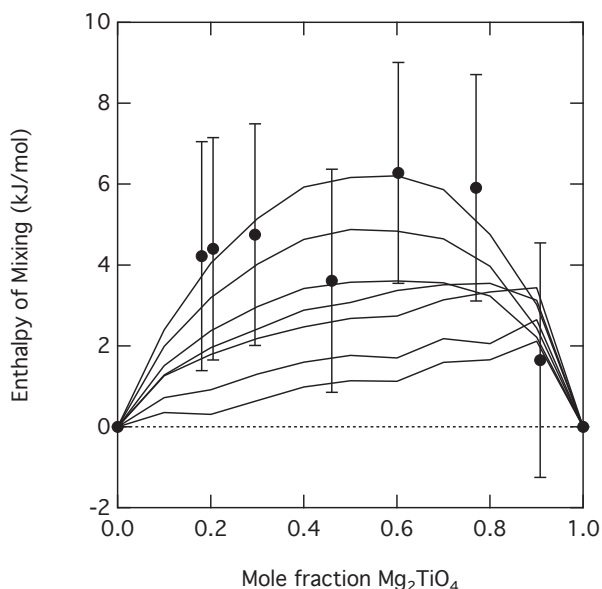


FIGURE 5. Enthalpy of mixing for MgFe_2O_4 - Mg_2TiO_4 calculated from MC simulations with $J_{\text{FeTi}}^{\text{TO}} = 1000$ K at temperatures of (from upper to lower curves) 1750, 1500, 1250, 1000, 750, 500, and 250 K. For comparison, data points show the measured enthalpy of mixing for Fe_3O_4 - Fe_2TiO_4 (Lilova et al. 2012).

behavior is similar to that observed in simulations of hematite-ilmenite (Harrison et al. 2000) and suggests the presence of a miscibility gap in the solid solution below ~ 1000 K. Evidence for chemical clustering driven by the positive value of $J_{\text{FeTi}}^{\text{TO}}$ can be seen in snapshots of the MC simulations (Fig. 6). Snapshots are shown for $M = 0.5$ with Mg^{2+} in red, Fe^{3+} in green, and Ti^{4+} in blue. At 1750 K there is a random distribution of MgFe_2O_4 (red/green) and Mg_2TiO_4 (red/blue) components throughout the simulation cell. At 1000 K and below the distribution becomes increasingly clustered into MgFe_2O_4 -rich and Mg_2TiO_4 -rich regions. The presence of a miscibility gap is also consistent with the thermodynamic model of Sack and Ghiorso (1991), who predicted an asymmetric gap below 883 K for MgFe_2O_4 - Mg_2TiO_4 .

COMPARISON WITH TITANOMAGNETITE

Cation distributions in titanomagnetite

A summary of recent experimental studies of cation ordering in titanomagnetite is shown in Figure 3b (Kačkol et al. 1991b; Hamdeh et al. 1999; Bosi et al. 2009; Pearce et al. 2010; Lilova et al. 2012). Unlike MgFe_2O_4 - Mg_2TiO_4 , there is considerable disagreement between different studies. Despite the scatter, however, some important trends emerge. For $M > 0.5$, the average trend falls close to the Akimoto/Random models, and there is reasonably good correspondence between the MgFe_2O_4 - Mg_2TiO_4 and Fe_3O_4 - Fe_2TiO_4 systems. For $0 \leq M \leq 0.5$, however, the data fall between the Akimoto and Néel-Chevalier models, with an average trend corresponding approximately to the Kačkol model. The range of scatter is consistent with the in situ measurements of Trestman-Matts et al. (1983), who found that the cation distribution tends toward the Akimoto model at high T and the

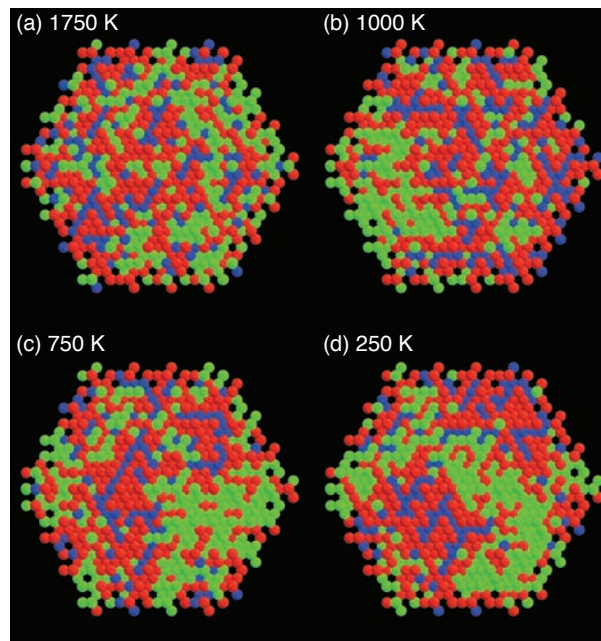


FIGURE 6. Snapshots of the final configuration of MC simulations performed for $M = 0.5$ and $T =$ (a) 1750 K, (b) 1000 K, (c) 750 K, and (d) 250 K. Mg^{2+} is red, Fe^{3+} is green, and Ti^{4+} is blue. View direction is [111]. (Color online.)

Néel-Chevalier model at low T . All of these data deviate markedly from MgFe₂O₄-Mg₂TiO₄ in the range $0 \leq M \leq 0.5$ (Fig. 3a), representing a fundamental difference in the behavior of the two systems.

On the basis of the available data, we suggest that MgFe₂O₄-Mg₂TiO₄ is a good analog of Fe₃O₄-Fe₂TiO₄ for $M > 0.5$. The analog breaks down, however, for $M \leq 0.5$. The analog between Mg and Fe²⁺ is well established for the end-members, both from experimental and modeling perspectives (Harrison and Putnis 1999a), with virtually identical values for Mg-Fe³⁺ and Fe²⁺-Fe³⁺ interaction parameters being determined by Palin and Harrison (2007b). Given the evidence for a large $J_{\text{FeTi}}^{\text{TO}}$ interaction in MgFe₂O₄-Mg₂TiO₄, and the similarity in enthalpies of mixing of the two systems (Fig. 5), we might also expect a $J_{\text{FeTi}}^{\text{TO}}$ interaction of similar magnitude in Fe₃O₄-Fe₂TiO₄. From Figure 2, however, it appears that values of $J_{\text{FeTi}}^{\text{TO}} < 500$ K are needed to reproduce cation distributions close to the Kákol model and even smaller values (≤ 250 K) are needed to reproduce the Néel-Chevalier model (as required, for example, by the data of Pearce et al. 2010). This breakdown points toward some fundamental aspects of the physical behavior of titanomagnetite that are not accounted for by our atomistic model in its current form. The presence of mobile, delocalized charge carriers in Fe₃O₄-rich titanomagnetite is likely to have a significant impact on the both the equilibrium and kinetic properties of the solid solution. Magnetic ordering may also play an important role at temperatures below 853 K. We now attempt to assess which factors, or combination of factors, can best account for the observed difference between MgFe₂O₄-Mg₂TiO₄ and Fe₃O₄-Fe₂TiO₄ for $M \leq 0.5$.

Coupling between cation ordering and magnetic ordering

Both Fe₃O₄ and MgFe₂O₄ adopt ferrimagnetic structures below their respective Curie temperatures (T_c). Whereas T_c for stoichiometric Fe₃O₄ is a constant 853 K, T_c for MgFe₂O₄ can lie anywhere in the range 550–700 K, depending on the degree of quenched-in cation disorder (O'Neill et al. 1992). Harrison and Putnis (1997) argued that cation ordering and magnetic ordering in MgFe₂O₄ are strongly coupled and that the coupling can be modeled successfully using a mean-field model. They included an energy term in the macroscopic free energy that links the two ordering processes: $E = \lambda x Q_m^2$, where Q_m is the magnetic order parameter and λ is a coupling constant. The sign of the coupling constant is such that an increase in the degree of inversion (x) causes an increase in the degree of magnetic order (i.e., T_c increases with x). Under conditions of global equilibrium with respect to x and Q_m , the opposite must also be true: i.e., when the degree of magnetic order increases on cooling through T_c we expect to see an enhanced degree of inversion. For MgFe₂O₄, the kinetics of cation ordering at $T = T_c$ are too slow to allow the onset of magnetic ordering to have any influence on the cation distribution (Harrison and Putnis 1999b). This is not the case for Fe₃O₄, however, where rapid redistribution of Fe²⁺ and Fe³⁺ can occur via electron hopping down to room temperature. Recent experimental observations of natural Fe₃O₄-Fe₂TiO₄ samples with $0.2 < M < 0.4$ (Bowles and Jackson, personal communication) provide strong evidence of coupling in the titanomagnetite solid solution.

In deriving the atomistic model we have taken no account of

coupling between cation and magnetic ordering processes below T_c . This is justifiable for MgFe₂O₄-Mg₂TiO₄, where kinetic limitations prevent global equilibrium with respect to x and Q_m from being achieved on laboratory timescales. It is possible, however, that coupling will lead to enhanced cation order in Fe₃O₄-Fe₂TiO₄, especially for $M < 0.5$, where $T_c > 600$ K and electron hopping is fast enough to respond to the magnetic transition. Incorporation of magnetic ordering into the atomistic model is an obvious next step (Harrison and Becker 2001; Harrison 2006), but is beyond the scope of the current study. Harrison and Putnis (1999a) applied the thermodynamic model of Harrison and Putnis (1997) to cation ordering data for Fe₃O₄ (Wißmann et al. 1998) and demonstrated that the mean-field approach correctly predicts the experimentally observed enhancement of cation order below T_c , implying that coupling in Fe₃O₄ is similar in strength to MgFe₂O₄. To demonstrate the magnitude of the effect, we have adapted the macroscopic approach of Harrison and Putnis (1997) to describe a system that behaves like MgFe₂O₄ in terms of its equilibrium cation ordering behavior, but like Fe₃O₄ in terms of its magnetic ordering and kinetic behavior. The total free energy of the system is written

$$\begin{aligned} G = & \alpha x + \beta x^2 & (4) \\ & + RT[x \ln(x) + (1-x) \ln(1-x) + x \ln(x/2) + (2-x) \ln(1-x/2)] \\ & + \frac{1}{2} a_m (T - T_c) Q_m^2 + \frac{1}{4} b_m Q_m^4 \\ & + \lambda x Q_m^2 \end{aligned}$$

where the first two lines represent the enthalpy and configurational entropy due to cation ordering (O'Neill and Navrotsky 1983), the third line represents the free energy due to magnetic ordering (Harrison and Putnis 1997), and the fourth line is the coupling term. Minimizing G with respect to Q_m at constant x yields

$$\begin{aligned} Q_m^2 = & \frac{b_m}{a_m} (T_c^* - T) & (5) \\ T_c^* = & T_c - \frac{2\lambda}{a_m} x \end{aligned}$$

which represents a second-order magnetic transition with re-normalized Curie temperature T_c^* that varies linearly with x . A value of $\lambda = -21\,059$ J/mol was obtained by fitting Equation 5 to the T_c - x data of O'Neill et al. (1992). A value of $T_c = 445$ K for the unrenormalized Curie temperature ensures that the equilibrium magnetic transition occurs at 853 K. Values of $\alpha = 26.6$ kJ/mol and $\beta = -21.7$ kJ/mol were taken from O'Neill et al. (1992). A value of $a_m = 86.35$ J/(mol·K) was calculated from the total magnetic entropy change for a Fe₃O₄-like material containing one Fe²⁺ and two Fe³⁺ cations [$\Delta S = 1/2 a_m = R(\ln 5 + 2 \ln 6)$]. A value of $b_m = 80\,542.5$ J/mol is required by the normalization condition ($Q_m = \pm 1$ at 0 K). The dashed line in Figure 7 shows the cation ordering behavior that would be observed in the absence of coupling to the magnetic transition. The enhancement of cation order due to coupling is shown by the thick solid line. The maximum difference between the two

curves is $\Delta x = 0.06$. Even if we make the generous assumption that magnetic ordering could influence the cation distribution by up to ~ 0.1 cations per formula unit, the effect is still a factor of ~ 2 too small to explain the discrepancy between average cation distributions in $\text{MgFe}_2\text{O}_4\text{-Mg}_2\text{TiO}_4$ and $\text{Fe}_3\text{O}_4\text{-Fe}_2\text{TiO}_4$. The ef-

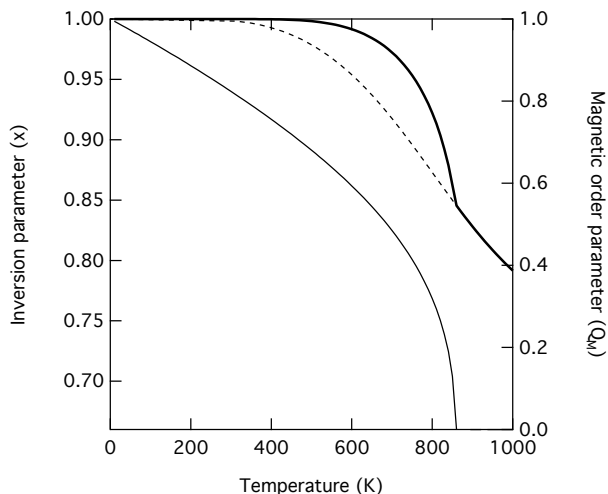


FIGURE 7. Prediction of how the degree of inversion ($x = \text{Fe}^{3+}$ on tetrahedral sites) is influenced by the onset of magnetic ordering in an inverse spinel with cation ordering behavior that is similar to MgFe_2O_4 but with magnetic ordering behavior that is similar to Fe_3O_4 . Thin dashed line (left axis) shows cation ordering behavior in the absence of coupling. Thick solid curve (left axis) shows the predicted behavior with coupling. Thin solid curve (right axis) shows the magnetic order parameter (Q_m).

fect is completely incapable of accounting for distributions that lie close to the Néel-Chevalier model (e.g., Pearce et al. 2010).

Compositional dependence of $J_{\text{FeTi}}^{\text{TO}}$

By adjusting the value of $J_{\text{FeTi}}^{\text{TO}}$, the atomistic model is capable of reproducing the entire range of proposed cation distribution models for titanomagnetite (Fig. 2). Any one particular model can be reproduced by relaxing the assumption that $J_{\text{FeTi}}^{\text{TO}}$ is a constant for all bulk compositions. To illustrate this concept we have determined the value of $J_{\text{FeTi}}^{\text{TO}}$ that is needed at each composition to obtain a cation distribution bounded at low T by the Kåkol model (Fig. 8a). This procedure yields a linear increase in $J_{\text{FeTi}}^{\text{TO}}$ from 250 K at $M = 0.2$ to 1100 K at $M = 0.9$ (closed circles in inset to Fig. 8a) and produces a good description of much of the published data.

Allowing $J_{\text{FeTi}}^{\text{TO}}$ to vary as a function of composition provides a powerful means of optimizing the parameters of the atomistic model to fit the experimental data. However, this fit is meaningless unless the compositional dependence can be physically justified. There are two main contributions to the cation-cation interaction parameters: a strain contribution resulting from size mismatch between cation pairs and an electrostatic contribution resulting from charge mismatch. Strain interactions can never be screened, and will always be present in a solid solution where cations of different size mix. In systems with large size mismatch (e.g., substitutions involving Mg^{2+} and Ca^{2+} —size mismatch $\sim 28\%$), it is sometimes necessary to include a composition dependent, configuration independent volume strain energy term when computing J parameters from static lattice energy calculations (Vinograd et al. 2004). In our case, however, Fe^{3+} and Ti^{4+} cations are similar in size (size mismatch $\sim 7\%$) but dif-

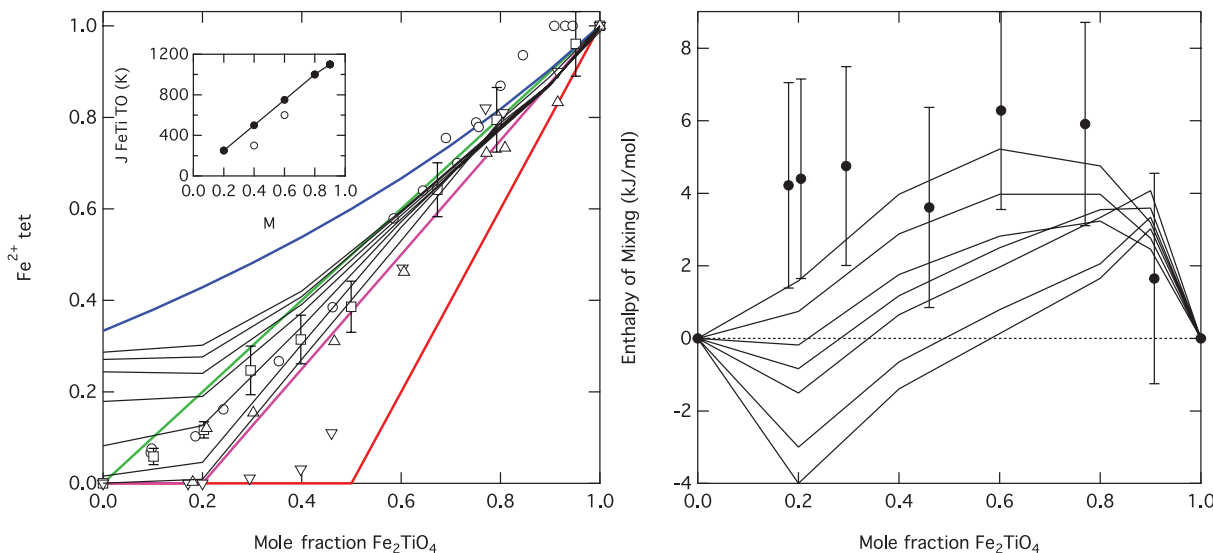


FIGURE 8. (a) Optimization of the atomistic model to reproduce the Kåkol model for $\text{Fe}_3\text{O}_4\text{-Fe}_2\text{TiO}_4$ (Kåkol et al. 1991b). Thin solid curves show the results of MC simulations with a value of $J_{\text{FeTi}}^{\text{TO}}$ that varies with composition according to the inset (solid circles). Simulations were performed for temperatures of (from upper to lower curves) 1750, 1500, 1250, 1000, 750, 500, and 250 K. Data are from Bosi et al. (2009) (circles), Hamdeh et al. (1999) (squares), Lilova et al. (2012) (upward triangles), and Pearce et al. (2010) (downward triangles). Thick solid lines show reference cation distribution models (from upper to lower): Random, Akimoto, Kåkol, and Néel-Chevalier. Open circles in the inset show values of $J_{\text{FeTi}}^{\text{TO}}$ that are needed to fit the data of Pearce et al. (2010). (b) Calculated enthalpy of mixing for $\text{Fe}_3\text{O}_4\text{-Fe}_2\text{TiO}_4$ using the cation distribution model from a. Data points show the measured enthalpy of mixing for $\text{Fe}_3\text{O}_4\text{-Fe}_2\text{TiO}_4$ (Lilova et al. 2012). (Color online.)

fer in charge, and electrostatic interactions are likely to make a larger contribution to $J_{\text{FeTi}}^{\text{TO}}$ than strain interactions. This is an important statement, since unlike strain interactions, electrostatic interactions may potentially be screened by mobile charge carriers. Figure 8a provides evidence that $J_{\text{FeTi}}^{\text{TO}}$ decreases linearly in proportion to the Fe_3O_4 content of the solid solution. We propose that the excess positive charge associated with octahedral Ti^{4+} is gradually screened by an increasing concentration of mobile charge carriers on the octahedral sublattice, thus reducing the electrostatic interaction of octahedral Ti^{4+} with tetrahedral Fe^{3+} in proportion to the Fe_3O_4 content of the solid solution. Sujata and Mason (1992) suggested a similar mechanism to explain the gradual reduction in the activation energy for cation redistribution in ferrospinels $(\text{Fe}_3\text{O}_4)_z(\text{MeFe}_2\text{O}_4)_{1-z}$ (Me = Co, Mn, Mg, Ni) with increasing Fe_3O_4 content. For example, the activation energy for Ni diffusion decreases steadily from 3.55 eV for $z = 0.03$ to 2.95 eV for $z = 0.14$, 2.6 eV for $z = 0.33$, and 2.08 eV for $z = 0.63$ (Eveno and Paulus 1974). Sujata and Mason (1992) argue that when the Fe_3O_4 content is large enough, small polaron hopping between Fe^{2+} and Fe^{3+} in ferrospinels can provide local electroneutrality for diffusing ionic species and can effectively screen these species during migration, thereby lowering the activation energy. Spinels that are unable to screen charge in this way display much larger activation energies, and in the case of MgFe_2O_4 adopt a very different mechanism of cation ordering (i.e., heterogeneous nucleation and growth instead of homogeneous local diffusion; Walters and Wirtz 1971; Kimura et al. 1977; Harrison and Putnis 1999b).

The proposed screening mechanism appears to be highly effective for compositions close to pure Fe_3O_4 , where $J_{\text{FeTi}}^{\text{TO}}$ is reduced to ~ 0 , making the solid solution virtually insensitive to dilute concentrations of Ti^{4+} on the octahedral sublattice. Note that screening of Ti^{4+} is preferred to a charge transfer mechanism, given the lack of any spectroscopic evidence for Ti^{3+} in the solid solution (Pearce et al. 2010). The reduced $J_{\text{FeTi}}^{\text{TO}}$ leads to a poorer agreement between the calculated and observed enthalpies of mixing (Fig. 8b), although the high- T curves are still within error of the experimental data and remain consistent with the presence of a miscibility gap in this system (Price 1981). The anomalous negative enthalpy of mixing for $M \sim 0.2$ is likely due to the fact that reducing $J_{\text{FeTi}}^{\text{TO}}$ means we no longer account properly for the volume strain energy contribution to the total energy. The agreement seen in Figure 5 could be restored, however, by addition of a small configuration independent strain energy term of the form suggested by Vinograd et al. (2004).

DISCUSSION

Comment on the merits of atomistic vs. macroscopic models

One of the most striking results of this study is the dramatic difference between atomistic and macroscopic models of cation ordering in MgFe_2O_4 - Mg_2TiO_4 (Fig. 4a). The O'Neill and Navrotsky (1983, 1984) model (from now on referred to as the O-N model) provides a near perfect description of cation ordering in end-member MgFe_2O_4 (O'Neill et al. 1992). Palin and Harrison (2007a) demonstrated from an atomistic perspective that the O-N model correctly captures the thermodynamic consequences

of cation ordering in end-member spinels (especially for normal spinels, where short-range order is limited), thereby explaining why it can be applied successfully to such a wide range of systems. It is somewhat surprising, therefore, that the O-N model fails to account for the rather simple linear relationship between Mg^{T} and M in the MgFe_2O_4 - Mg_2TiO_4 solid solution (Fig. 3a). Below we consider possible reasons for the difference between the atomistic and macroscopic approaches to modeling this system, with implications for other systems of this type.

In the O-N model of MgFe_2O_4 - Mg_2TiO_4 , cation ordering in the solid solution is defined by the two energy parameters α and β (Eq. 3). These two parameters are entirely constrained by cation ordering behavior in MgFe_2O_4 ; no parameters specific to the solid solution enter the cation distribution model. The mixing properties of the solid solution are defined by a regular solution term of the form $\Delta H_{\text{mix}} = WM(1 - M)$ that depends only on bulk composition. The adjustable parameter W allows the enthalpy of mixing and appearance of miscibility gaps to be described, but it does not influence the calculated cation distributions in any way. The parameterization of the atomistic model is also heavily constrained by cation ordering behavior in the end-members. In this study we chose to fix $J_{\text{MgFe}}, J_{\text{MgTi}}, \mu_x$, and μ_y at their end-member values (a procedure that is equivalent to using end-member values of α and β in the O-N model). Inspired by the results of static lattice energy calculations, the mixing properties of the solid solution were then defined by $J_{\text{FeTi}}^{\text{TO}}$. This single adjustable parameter plays a similar role to W in the O-N model, in that it directly influences the enthalpy of mixing and appearance of miscibility gaps (Fig. 5). However, unlike W , $J_{\text{FeTi}}^{\text{TO}}$ also influences the cation distribution in two distinct ways. First, a positive $J_{\text{FeTi}}^{\text{TO}}$ drives the system to avoid Fe^{3+} - Ti^{4+} T-O pairs. Since Ti^{4+} is strongly partitioned onto O sites, the system can reduce its total energy by replacing Fe^{3+} on T with Mg^{2+} . This substitution will only occur when the resulting energy reduction outweighs the increase in chemical potential energy (μ_x). The energy balance tips in favor of increased Mg^{T} for $J_{\text{FeTi}}^{\text{TO}} \geq 500$ K (Fig. 2). Second, a positive $J_{\text{FeTi}}^{\text{TO}}$ drives the system to chemically cluster and eventually unmix (Fig. 6). In the limit of perfect unmixing into a mechanical mixture of inverse MgFe_2O_4 and inverse Mg_2TiO_4 , the amount of Mg^{2+} on tetrahedral sites (averaged over the whole simulation cell) would be $\text{Mg}^{\text{T}} = M$ (i.e., the Akimoto model). This may help to explain why the system evolves toward the Akimoto model with increasing $J_{\text{FeTi}}^{\text{TO}}$, and suggests that the short-range chemical clustering observed in Figure 6 may be a prerequisite to obtaining the correct cation distribution. Such short-range effects can only be described using the atomistic approach, providing additional motivation for the continued development of such models.

Outlook

This comparative study of MgFe_2O_4 - Mg_2TiO_4 and Fe_3O_4 - Fe_2TiO_4 has highlighted several issues that need to be more thoroughly investigated before a complete model of the titanomagnetite system can be finalized. The proposed screening mechanism, whereby the electrostatic contribution to certain cation-cation interaction energies can be reduced in proportion to the Fe_3O_4 content of the solid solution, needs to be confirmed. A possible methodology would be to perform detailed first-principles ab initio calculations, where the assumption of discrete Fe^{2+} and Fe^{3+} cations with formal

charges can be relaxed and the excess electronic charge can be allowed to distribute itself more naturally across the available Fe sites (Pentcheva and Nabi 2008; Nabi et al. 2010; Skomurski et al. 2010). Any new analysis of this type should also investigate in more detail the relative importance of electrostatic vs. volume strain contributions to the total energy, so that the final model can reproduce observed cation distributions and enthalpies of mixing simultaneously (Vinograd et al. 2004). We have shown that coupling between magnetic and cation ordering will have a small but non-negligible effect on the cation distribution below T_c , and therefore including coupling is a necessary next step in improving the atomistic model. The temperature- and composition-dependent kinetics of Fe^{2+} - Fe^{3+} redistribution in titanomagnetite are poorly constrained. Kinetic effects play a crucial role in understanding the impact of coupling to the magnetic transition and also in helping to explain the large variation in observed cation distributions between different experimental studies. Kinetic studies of synthetic and natural titanomagnetite are, therefore, a crucial area for future experimental work.

ACKNOWLEDGMENTS

This work was supported by the European Science Foundation (ESF) under the EUROCORES program EuroMinSci, through contract number ERASCT-2003-980409 of the European Commission, DG Research, FP6, and through NERC Grant NE/D522203/1.

REFERENCES CITED

- Akimoto, S. (1954) Thermomagnetic study of ferromagnetic minerals contained in igneous rocks. *Journal of Geomagnetism and Geoelectricity*, 6, 1–14.
- Andreozzi, G.B. and Lucchesi, S. (2002) Intersite distribution of Fe^{2+} and Mg in the spinel (sensu stricto)-hercynite series by single-crystal X-ray diffraction. *American Mineralogist*, 87, 1113–1120.
- Antao, S.M., Hassan, I., and Parise, J.B. (2005) Cation ordering in magnesioferrite, MgFe_2O_4 to 982 °C using in situ synchrotron X-ray powder diffraction. *American Mineralogist*, 90, 219–228.
- Bosenick, A., Dove, M.T., Myers, E.R., Palin, E.J., Sainz-Diaz, C.I., Guiton, B.S., Warren, M.C., Craig, M.S., and Redfern, S.A.T. (2001) Computational methods for the study of energies of cation distributions: Applications to cation-ordering phase transitions and solid solutions. *Mineralogical Magazine*, 65, 193–219.
- Bosi, F., Hälenus, U., and Skogby, H. (2009) Crystal chemistry of the magnetite-ulvöspinel series. *American Mineralogist*, 94, 181–189.
- Chevalier, R., Bofa, J., and Mathieu, S. (1955) Titanomagnétites et ilménites ferromagnétiques. *Bulletin du Société Française Minéralogie et Cristallographie*, 78, 307–346.
- Church, N., Feinberg, J., and Harrison, R.J. (2011) Low-temperature domain wall pinning in titanomagnetite. *Geochemistry Geophysics Geosystems*, 12, Q07Z27, doi:10.1029/2011GC003538.
- de Grave, E., de Sitter, J., and Vandenberghe, R. (1975) On the cation distribution in the spinel system $y\text{Mg}_2\text{TiO}_4$ -(1-y) MgFe_2O_4 . *Applied Physics*, 7, 77–80.
- Eveno, P. and Paulus, M. (1974) Diffusion of nickel-63 in mixed ferrites of iron and nickel. *Physica status solidi (a)*, 22, 569–577.
- Gale, J.D. (1997) GULP: A computer program for the symmetry-adapted simulation of solids. *Journal of the Chemical Society: Faraday Transactions*, 93, 629–637.
- Gale, J.D. and Rohl, A.L. (2003) The general utility lattice program (GULP). *Molecular Simulation*, 29, 291–341.
- Hamdeh, H.H., Barghout, K., Ho, J.C., Shand, P.M., and Miller, L.L. (1999) A Mössbauer evaluation of cation distribution in titanomagnetites. *Journal of Magnetism and Magnetic Materials*, 191, 72–78.
- Harrison, R.J. (2006) Microstructure and magnetism in the ilmenite-hematite solid solution: a Monte Carlo simulation study. *American Mineralogist*, 91, 1006–1024.
- Harrison, R.J. and Becker, U. (2001) Magnetic ordering in solid solutions. In C. Geiger, Ed., *Solid Solutions in Silicate and Oxide Systems*, 3, Ch. 13, 349–383. European Mineralogical Union Notes in Mineralogy, Eötvös University Press, Budapest.
- Harrison, R.J. and Putnis, A. (1997) The coupling between magnetic and cation ordering: A macroscopic approach. *European Journal of Mineralogy*, 9, 1115–1130.
- (1999a) The magnetic properties and crystal chemistry of oxide spinel solid solutions. *Surveys in Geophysics*, 19, 461–520.
- (1999b) Determination of the mechanism of cation ordering in magnesioferrite (MgFe_2O_4) from the time- and temperature-dependence of magnetic susceptibility. *Physics and Chemistry of Minerals*, 26, 322–332.
- Harrison, R.J., Becker, U., and Redfern, S.A.T. (2000) Thermodynamics of the R-3 to R-3c phase transition in the ilmenite-hematite solid solution. *American Mineralogist*, 85, 1694–1705.
- Kakol, Z., Sabol, J., and Honig, J. (1991a) Magnetic anisotropy of titanomagnetites $\text{Fe}_{3-x}\text{Ti}_x\text{O}_4$ ($0 \leq x < 0.55$). *Physical Review B: Condensed Matter*, 44, 2198–2204.
- (1991b) Cation distribution and magnetic properties of titanomagnetites $\text{Fe}_{3-x}\text{Ti}_x\text{O}_4$ ($0 \leq x < 1$). *Physical Review B: Condensed Matter*, 43, 649–654.
- Kimura, T., Ichikawa, M., and Yamaguchi, T. (1977) Effects of grain size on cation ordering in sintered Mg-ferrites. *Journal of Applied Physics*, 48, 5033–5037.
- Lilova, K.I., Pearce, C., Gorski, C., Rosso, K.M., and Navrotsky, A. (2012) Thermodynamics of the magnetite-ulvöspinel (Fe_3O_4 - Fe_2TiO_4) solid solution. *American Mineralogist*, 97, 1330–1338.
- Nabi, H.S., Harrison, R.J., and Pentcheva, R. (2010) Magnetic coupling parameters at an oxide-oxide interface from first principles: Fe_2O_3 - FeTiO_3 . *Physical Review B*, 81, 214432.
- Néel, L. (1955) Some theoretical aspects of rock-magnetism. *Advances in Physics*, 54, 191–243.
- Nell, J., Wood, B., and Mason, T.O. (1989) High-temperature cation distributions in Fe_3O_4 - MgAl_2O_4 - MgFe_2O_4 - FeAl_2O_4 spinels from thermopower and conductivity measurements. *American Mineralogist*, 74, 339–351.
- O'Neill, H.St.C. and Navrotsky, A. (1983) Simple spinels: Crystallographic parameters, cation radii, lattice energies, and cation distribution. *American Mineralogist*, 68, 181–194.
- (1984) Cation distributions and thermodynamic properties of binary spinel solid solutions. *American Mineralogist*, 69, 733–753.
- O'Neill, H.St.C., Annersten, H., and Virgo, D. (1992) The temperature dependence of the cation distribution in magnesioferrite (MgFe_2O_4) from powder XRD structural refinements and Mössbauer spectroscopy. *American Mineralogist*, 77, 725–740.
- O'Neill, H.St.C., Redfern, S.A.T., Kesson, S., and Short, S. (2003) An in situ neutron diffraction study of cation disordering in synthetic qandilite Mg_2TiO_4 at high temperatures. *American Mineralogist*, 88, 860–865.
- Palin, E.J. and Harrison, R.J. (2007a) A computational investigation of cation ordering phenomena in the binary spinel system MgAl_2O_4 - FeAl_2O_4 . *Mineralogical Magazine*, 71, 611–624.
- (2007b) A Monte Carlo investigation of the thermodynamics of cation ordering in 2-3 spinels. *American Mineralogist*, 92, 1334–1345.
- Palin, E.J., Walker, A.M., and Harrison, R.J. (2008) A computational study of order-disorder phenomena in Mg_2TiO_4 spinel (qandilite). *American Mineralogist*, 93, 1363–1372.
- Pearce, C., Henderson, C.M.B., Telling, N.D., Patrick, R.A.D., Charnock, J.M., Coker, V.S., Arenholz, E., Tuna, F., and van der Laan, G. (2010) Fe site occupancy in magnetite-ulvöspinel solid solutions: A new approach using X-ray magnetic circular dichroism. *American Mineralogist*, 95, 425–439.
- Pentcheva, R. and Nabi, H.S. (2008) Interface magnetism in Fe_3O_4 / FeTiO_3 heterostructures. *Physical Review B*, 77, 172405.
- Price, G.D. (1981) Subsolidus phase relations in the titanomagnetite solid solution series. *American Mineralogist*, 66, 751–758.
- Sack, R.O. and Ghiorso, M.S. (1991) An internally consistent model for the thermodynamic properties of Fe-Mg-titanomagnetite-aluminate spinels. *Contributions to Mineralogy and Petrology*, 106, 474–505.
- Skomurski, F.N., Kerisit, S.N., and Rosso, K.M. (2010) Structure, charge distribution, and electron hopping dynamics in magnetite (Fe_3O_4) (100) surfaces from first principles. *Geochimica et Cosmochimica Acta*, 74, 4234–4248.
- Sujata, K. and Mason, T.O. (1992) Kinetics of cation redistribution in ferrosinels. *Journal of the American Ceramic Society*, 75, 557–562.
- Tellier, J.C. (1967) Sur la substitution dans le ferrite de magnésium des ions ferriques par les ions trivalents, tetravalent et pentavalent. *Revue de Chimie Minérale*, 4, 325–365.
- Trestman-Matts, A., Dorris, S.E., Kumarakrishnan, S., and Mason, T.O. (1983) Thermoelectric determination of cation distributions in Fe_3O_4 - Fe_2TiO_4 . *Journal of the American Ceramic Society*, 66, 829–834.
- Trestman-Matts, A., Dorris, S.E., and Mason, T.O. (1984) Thermoelectric determination of cation distributions in Fe_3O_4 - MgFe_2O_4 . *Journal of the American Ceramic Society*, 67, 69–73.
- Vinograd, V.L., Sluiter, M.H.F., Winkler, B., Putnis, A., Hälenus, U., Gale, J.D., and Becker, U. (2004) Thermodynamics of mixing and ordering in pyrope-grossular solid solution. *Mineralogical Magazine*, 68, 101–121.
- Walters, D.S. and Wirtz, G.P. (1971) Kinetics of cation ordering in magnesium ferrite. *Journal of the American Ceramic Society*, 54, 563–566.
- Wißmann, S., Wurm, V. v., Litterst, F.J., Dieckmann, R., and Becker, K.D. (1998) The temperature-dependent cation distribution in magnetite. *Journal of Physics and Chemistry of Solids*, 59, 321–330.